Applied Acoustics 72 (2011) 975–981

Contents lists available at ScienceDirect

Applied Acoustics

journal homepage: www.elsevier.com/locate/apacoust

Technical Note

Dynamic characterization of beam type structures: Analytical, numerical and experimental applications

Paul H. Kohan [a,b,*], Liz G. Nallim [a,b], Susana B. Gea [a]

[a] ICMASa, Facultad de Ingeniería, UNSa (Universidad Nacional de Salta), Av. Bolivia 5150, 4400 Salta, Argentina
[b] INIQUI (CONICET), Av. Bolivia 5150, 4400 Salta, Argentina

ARTICLE INFO

Article history:
Received 15 July 2010
Received in revised form 4 March 2011
Accepted 13 June 2011
Available online 7 July 2011

Keywords:
Timoshenko beams
Dynamic characterization
Ritz method
Ambent vibration test

ABSTRACT

A general algorithm for the free vibration analysis of stepped and tapered beam type structures with multiple elastic supports is developed in this work. The analytical formulation is based on the Ritz method and on the use of orthogonal polynomials within the framework of the first order shear deformation beam theory. To verify the validity and convergence of the general algorithm several numerical examples are analyzed. A further example concerned with the determination of the dynamical properties of a bell tower is also presented and compared with the finite element method and experimental results.
© 2011 Elsevier Ltd. All rights reserved.

1. Introduction

Several structures typically used in practice engineering can be represented as multispan beams, being the development of modeling tools for the study of the dynamic behavior of these structures of great interest. The finite element method allows representing with great detail the geometric dimensions of a structure, the stiffness and mass distributions obtaining realistic numerical, but involving a high computational cost. This computational work increases, when different complicating effects such as stepped or tapered cross sections are included. In addition, continuous models may imply more complex considerations in the formulation but, in general, require less computational work and less time computational preprocessing for their resolution.

Several methods have been developed to investigate the free vibrational response of Timoshenko beams. Farlghaly [1] presents an analytical study of a system of elastically supported multi-span uniform Timoshenko beams in which the beam system is loaded with end as well as intermediate concentrated masses. Relative span and relative thickness parameters are defined and included in the analytical formulation allowing the determination of natural frequencies of stepped beams. Although the exact natural frequencies for systems of two and three spans have been computed, the analytical procedure requires a particular solution for each case. Tong et al. [2] presents the step-reduction method to analyze the free vibrations of tapered beams which is based on replacing the non-homogeneous beam with variable cross section by a number of homogeneous stepped beams with constant cross-section. Lin and Chang [3] analyze the free vibration of a multi-span Timoshenko beam with an arbitrary number of flexible constraints by considering the compatibility requirements on each constraint point and using a transfer matrix method. Lin [4–6] determined the natural frequencies and mode shapes of uniform Bernoulli and Timoshenko multi-span beams carrying a number of various concentrated elements including masses and springs.

The present work is oriented to the development of computational tools that can be used to analyze the dynamic behavior of beam type structural elements. Following this objective, a general algorithm to determine the dynamical behavior of variable thickness thick beam structures, based on the Ritz method, is developed generalizing and extending the methodology proposed by Nallim and Grossi [7] for Bernoulli beam analysis. This analytical formulation uses characteristic orthogonal polynomials as approximating functions [8] and allows the study of beams with various complicating effects such as stepped and tapered cross sections, presence of arbitrarily placed concentrated masses and different support conditions, including elastic rotational and translational constraints. In addition, the problem is solved considering the shear strains through the Timoshenko theory for thick beams. In order to validate the algorithm and its computational implementation, natural frequencies for different cases presented by Rossi et al. [9] and by Tong et al. [2] are compared with results obtained using the proposed formulation and three-dimensional finite element models.

* Corresponding author at: ICMASa, Facultad de Ingeniería, UNSa (Universidad Nacional de Salta), Av. Bolivia 5150, 4400 Salta, Argentina.
E-mail address: paulkohan@unsa.edu.ar (P.H. Kohan).

0003-682X/$ - see front matter © 2011 Elsevier Ltd. All rights reserved.
doi:10.1016/j.apacoust.2011.06.007

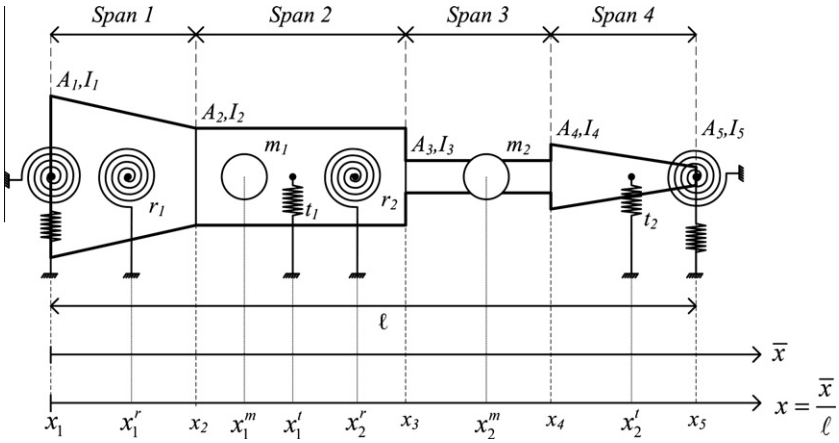

Fig. 1. Beam with different complicating effects.

Finally, the proposed algorithm is used for the analysis of the bell tower of the church Nuestra Señora de la Candelaria de la Viña placed in Salta city (Argentina). The model was calibrated with experimental measurements of natural frequencies under environmental vibration [10–13]. The results determined using the present method are compared with results from a three-dimensional finite element model, showing that the computational work needed to solve the problem is considerable lower.

2. Proposed algorithm for dynamic study of beams

The proposed algorithm for the dynamic study of beams is based on the Ritz method, using the orthogonal polynomial shape functions proposed by Bhat [8]. In a previous work, Nallim and Grossi [7] developed a general algorithm to determine the natural frequencies of beams with several complicating effects, including variable thickness, presence of an arbitrarily placed concentrated mass and different end conditions. This previous work is now extended and generalized considering the shear strains through the incorporation of the Timoshenko theory for thick beams, variable stepped and tapered cross sections, and also the presence of elastic restraints at arbitrary positions (see Fig. 1). In these cases, the strain energy U_b and kinetic energy T of a beam are given respectively by:

$$U_b = \int_0^{\ell} \left\{ \frac{EI(\bar{x})}{2} \left[\frac{\partial \psi(\bar{x},t)}{\partial \bar{x}} \right]^2 + \frac{\kappa GA(\bar{x})}{2} \left[\psi(\bar{x},t) - \frac{\partial w(\bar{x},t)}{\partial \bar{x}} \right]^2 \right\} d\bar{x} \quad (1)$$

$$T = \int_0^{\ell} \left\{ \frac{\rho A(\bar{x})}{2} \left[\frac{\partial w(\bar{x},t)}{\partial t} \right]^2 + \frac{\rho I(\bar{x})}{2} \left[\frac{\partial \psi(\bar{x},t)}{\partial t} \right]^2 \right\} d\bar{x} \quad (2)$$

where ℓ is the total length of the beam, $A(\bar{x})$ is the cross-sectional area, ρ is the material density, $I(\bar{x})$ the moment of inertia, $w(\bar{x},t)$ is the transverse displacement and $\psi(\bar{x},t)$ is the rotation of the beam sections.

Let us consider the beam shown in Fig. 1, defined by a number N_s of spans. To simplify the theoretical framework the dimensionless variable $x = \frac{\bar{x}}{\ell}$ is introduced. The ends of the beam can be elastically restrained against rotation and translation and classical end conditions (free, simply supported or clamped) can be generated as particular cases. Also, rotational springs t and translational springs s attached to the beam in different points are considered in the analysis. Each beam span q is defined between coordinates x_q and x_{q+1} ($q = 1, \ldots, N_s$). The longitudinal elastic modulus E_q, shear modulus G_q, density ρ_q and the shear correction factor κ_q are constant in each span, while the area $A_q(x)$ and moment of inertia $I_q(x)$ may vary linearly. Therefore, considering a beam with rectangular cross section with width $b_q(x)$ and depth $h_q(x)$, it is possible to define the corresponding variable area and moment of inertia though the next set of equations:

$$h_q(x) = h_q[1 + c_{hq}(x - x_q)], \quad c_{hq} = \frac{h_{q+1}}{h_q} - 1 \quad (3)$$

$$b_q(x) = b_q[1 + c_{bq}(x - x_q)], \quad c_{bq} = \frac{b_{q+1}}{b_q} - 1 \quad (4)$$

$$I_q(x) = \frac{b_q(x)h_q^3(x)}{12} = I_q[1 + c_{bq}(x - x_q)][1 + c_{hq}(x - x_q)]^3,$$
$$I_q(x) = \alpha_q(x) I_q, \quad I_q = \frac{b_q h_q^3}{12} \quad (5)$$

$$A_q(x) = b_q(x)h_q(x) = A_q[1 + c_{bq}(x - x_q)][1 + c_{hq}(x - x_q)],$$
$$A_q(x) = \beta_q(x) A_q, \quad A_q = b_q h_q \quad (6)$$

In free vibrations of the beam, the transverse deflection $w(x,t)$ and the normal rotation of $\psi(x,t)$ can be expressed as:

$$w(x,t) = W(x)e^{i\omega t} \quad \psi(x,t) = \Psi(x)e^{i\omega t} \quad (7)$$

where $W(x)$ and $\Psi(x)$ are the amplitudes defined by approximation functions and ω is the angular frequency. Each approximating function must be continuous, have a continuous first derivative, and must satisfy the geometric boundary conditions of the system. Based on the work of Bhat [8] and Nallim and Grossi [7], the approximation functions are defined by:

$$W(x) = \sum_{i=1}^{n} c_i p_i(x) \quad \Psi(x) = \sum_{i=1}^{n} d_i \frac{\varphi_i(x)}{\ell} \quad (8)$$

where c_i and d_i are arbitrary coefficients to be determined and $p_i(x)$ and $\varphi_i(x)$ are sets of n orthogonal polynomials. The process to assemble the orthogonal polynomials is detailed in Nallim and Grossi [7].

For the beam depicted in Fig. 1 and taking into account Eq. (7), the maximum strain energy is expressed as:

$$U_{\max} = U_{b,\max} + U_{r,\max} + U_{t,\max} \quad (9)$$

where $U_{b,\max}$ is the maximum strain energy due to bending of the beam, $U_{r,\max}$ is the maximum strain energy of rotational springs and $U_{t,\max}$ is the maximum strain energy of translational springs.

Considering the maximum shear strains, the strain energy of the beam is obtained using Eqs. (1) and (7) as

$$U_{b,\max} = \frac{E_1 I_1}{2\ell}\sum_{q=1}^{N_s}\int_{x_q}^{x_{q+1}}\left\{\alpha_q(x)\theta_q^{Ub1}\left[\frac{\partial\Psi(x)}{\partial x}\right]^2\right\}dx + \frac{\kappa_1 G_1 A_1 \ell}{2} \times \sum_{q=1}^{N_s}\int_{x_i}^{x_{i+1}}\left\{\beta_q(x)\theta_q^{Ub2}\left[\Psi(x) - \frac{1}{\ell}\frac{\partial W(x)}{\partial x}\right]^2\right\}dx \quad (10)$$

where $\theta_q^{Ub1} = \frac{E_q I_q}{E_1 I_1}$ and $\theta_q^{Ub2} = \frac{\kappa_q G_q A_q}{\kappa_1 G_1 A_1}$.

The maximum strain energies associated with the deformation of the rotational springs and translational springs result:

$$U_{r,\max} = \frac{r_1}{2\ell^2}\sum_{j=1}^{Nr}\theta_j^{rot}\left[\Psi\left(x_j^r\right)\right]^2 \quad (11)$$

$$U_{t,\max} = \frac{t_1}{2}\sum_{j=1}^{Nt}\theta_j^{tras}\left[W\left(x_j^t\right)\right]^2 \quad (12)$$

where r_j and t_j are the jth rotational and translational spring constants, N_r and N_t are the total number of each type of springs with $\theta_j^{rot} = \frac{r_j}{r_1}$ and $\theta_j^{tras} = \frac{t_j}{t_1}$.

The maximum kinetic energy of the beam is given by:

$$T_{b,\max} = \frac{\ell^3}{2}\rho_1 A_1 \omega^2\left\{\sum_{q=1}^{Ns}\int_{x_q}^{x_{q+1}}\left[\frac{1}{\ell^2}\beta_q(x)\theta_q^{Tb2}W^2(x)\right]dx + \eta_1\sum_{q=1}^{Ns}\int_{x_q}^{x_{q+1}}\left[\alpha_q(x)\theta_q^{Tb2}\Psi^2(x)\right]dx\right\} \quad (13)$$

where $\theta_q^{Tb1} = \frac{\rho_q A_q}{\rho_1 A_1}$, $\eta_1 = \frac{I_1}{A_1\ell^2}$ and $\theta_q^{Tb2} = \frac{\rho_q I_q}{\rho_1 I_1}$.

Finally, the maximum kinetic energy of the attached masses is given by:

$$T_{m,\max} = \frac{1}{2}m_1\omega^2\left[\sum_{j=1}^{Nm}\theta_j^m W^2(x_j^m)\right] \quad (14)$$

where m_i is the magnitude of the ith attached mass, N_m is the total number of masses attached and $\theta_j^m = \frac{m_j}{m_1}$.

The Rayleigh quotient for the analyzed mechanical system is defined by the following expression:

$$\Omega^2 = \frac{\rho_1 A_1}{E_1 I_1}\ell^4\omega^2 = \frac{I_{U1} + \gamma I_{U2} + R I_{Rot} + T I_{Tras}}{I_{T1} + \eta_1 I_{T2} + \eta_2 I_m} \quad (15)$$

where

$$I_{U1} = \sum_{i=1}^{Ns}\int_{x_q}^{x_{q+1}}\left\{\alpha_q(x)\theta_q^{Ub1}\left[\frac{\partial\Psi(x)}{\partial x}\right]^2\right\}dx,$$

$$I_{U2} = \sum_{i=1}^{Ns}\int_{x_q}^{x_{q+1}}\left\{\beta_q(x)\theta_i^{Ub2}\left[\Psi(x) - \frac{1}{\ell}\frac{\partial W(x)}{\partial x}\right]^2\right\}dx$$

$$I_{T1} = \sum_{q=1}^{Ns}\int_{x_q}^{x_{q+1}}\left[\frac{1}{\ell^2}\beta_q(x)\theta_q^{Tb1}W^2(x)\right]dx,$$

$$I_{T2} = \sum_{q=1}^{Ns}\int_{x_q}^{x_{q+1}}\left[\alpha_q(x)\theta_q^{Tb2}\Psi^2(x)\right]dx$$

$$I_{Rot} = \frac{1}{\ell^2}\sum_{j=1}^{Nr}\theta_j^{rot}\left[\frac{\partial W(x_j^r)}{\partial x}\right]^2, \quad I_{Tras} = \sum_{j=1}^{Nt}\theta_j^{tras}\left[W\left(x_j^t\right)\right]^2,$$

$$I_m = \sum_{j=1}^{Nm}\frac{1}{\ell^2}\theta_j^m\left[W\left(x_j^m\right)\right]^2$$

$$\eta_2 = \frac{m_1}{\rho_1 A_1 \ell}, \quad \gamma = \frac{\kappa_1 G_1 A_1}{E_1 I_1}\ell^2, \quad R = \frac{r_1}{E_1 I_1}\ell, \quad T = \frac{t_1}{E_1 I_1}\ell^3$$

The expression of Ω^2 in Eq. (15) is, therefore, depending on the parameters c_i and d_i that have been introduced in this equation due to the assumed shape functions. The necessary condition for the minimization of Ω^2 with respect to the coefficients c_i and d_i are $\frac{\partial\Omega^2}{\partial c_i} = 0$ and $\frac{\partial\Omega^2}{\partial d_i} = 0$. From these two conditions the following system of $2n$ equations is obtained:

$$\begin{bmatrix}[K^{WW}] & [K^{W\Psi}]\\ [K^{\Psi W}] & [K^{\Psi\Psi}]\end{bmatrix}\begin{Bmatrix}\{c\}\\ \{d\}\end{Bmatrix} - \Omega^2\begin{bmatrix}[M^{WW}] & [0]\\ [0] & [M^{\Psi\Psi}]\end{bmatrix}\begin{Bmatrix}\{c\}\\ \{d\}\end{Bmatrix} = \begin{Bmatrix}\{0\}\\ \{0\}\end{Bmatrix} \quad (16)$$

where

$$K_{k,L}^{WW} = \sum_{L=1}^{n}\left[\gamma\sum_{q=1}^{Ns}\theta_q^{Ub2}\int_{x_q}^{x_{q+1}}\beta_q(x)p_L'(x)p_k'(x) + T\sum_{j=1}^{Nt}\theta_j^{tras}p_L\left(x_j^{tras}\right)p_k\left(x_j^{tras}\right)\right]$$

$$K_{k,L}^{W\Psi} = \sum_{L=1}^{n}\left[-\gamma\sum_{q=1}^{Ns}\theta_q^{Ub2}\int_{x_q}^{x_{q+1}}\beta_q(x)\varphi_L(x)p_k'(x)\right]$$

$$K_{k,L}^{\Psi W} = \sum_{L=1}^{n}\left[-\gamma\sum_{q=1}^{Ns}\theta_q^{Ub2}\int_{x_q}^{x_{q+1}}\beta_q(x)p_L'(x)\varphi_k(x)\right]$$

$$K_{k,L}^{\Psi\Psi} = \sum_{L=1}^{n}\left[\sum_{q=1}^{Ns}\theta_q^{Ub1}\int_{x_q}^{x_{q+1}}\alpha_q(x)\varphi_L'(x)\varphi_k'(x) + \gamma\sum_{q=1}^{Ns}\theta_q^{Ub2}\int_{x_q}^{x_{q+1}}\beta_q(x)\varphi_L(x)\varphi_k(x) + R\sum_{j=1}^{Nr}\theta_j^{rot}\varphi_L\left(x_j^{rot}\right)\varphi_k\left(x_j^{rot}\right)\right]$$

$$M_{k,L}^{WW} = \sum_{L=1}^{n}\left[\sum_{q=1}^{Ns}\theta_q^{Tb1}\int_{x_q}^{x_{q+1}}\beta_q(x)p_L(x)p_k(x) + \eta_2\sum_{j=1}^{Nm}\theta_j^m p_L\left(x_j^m\right)p_k\left(x_j^m\right)\right]$$

$$M_{k,L}^{\Psi\Psi} = \sum_{L=1}^{n}\left[\eta_1\sum_{q=1}^{Ns}\theta_q^{Tb2}\int_{x_q}^{x_{q+1}}\alpha_q(x)\varphi_L(x)\varphi_k(x)\right]$$

The solution of Eq. (16) leads to the following eigenvalue problem:

$$[K]\{z\} = \Omega^2[M]\{z\} \quad (17)$$

The solution of Eq. (17) results in approximations to the first n natural free vibration frequencies of the mechanical system. Finally, if the cross sections of the beam in each span are constant the functions $\alpha_q(x)$ and $\beta_q(x)$ are eliminated from the Eq. (16).

3. Convergence analysis

The results summarized in Table 1 are used to analyze the convergence of eigenfrequencies based on the number of coordinate functions employed for the deflection and rotation. All results presented correspond to the natural frequencies of a rectangular cross section cantilever beam with a length–hight ratio equal to 10. For comparison purpose, results of finite element method using 3D solid elements in SAP2000 [14] are also included in Table 1. It is observed that for the frequencies associated with the lower modes, convergence is achieved using a smaller number of orthogonal polynomials than for the higher modes. In addition, results with reasonable accuracy are obtained, at least to the third mode, using 8 polynomials.

Table 1
Dimensionless natural frequencies used for convergence analysis.

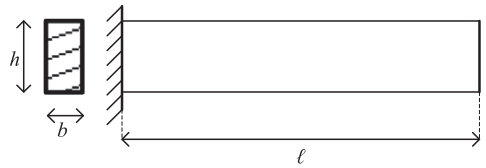

$b = 0.5\ h$ $\quad k = 5/6$ $\quad \nu = 0.3$

$\Omega_i = (\sqrt{\rho_1 A_1 L^4/E_1 I_1})\omega_i$
$\eta_1 = \frac{I_1}{A_1 \ell^2} \therefore h_1 = \sqrt{12\eta_1}\ell$
$\sqrt{\eta_1} = \frac{1}{1200}$

Freq.	Sap2000 3D model	Results using the algorithm according to the number of polynomials							
		2	4	6	7	8	9	10	11	12
Ω_1	3.5355	4.3900	3.4897	3.4884	3.4884	3.4884	3.4884	3.4884	3.4884	3.4884
Ω_2	21.2042	51.8700	21.0019	20.9071	20.9070	20.9069	20.9069	20.9069	20.9069	20.9069
Ω_3	55.8402		79.8207	55.5640	54.9953	54.9928	54.9884	54.9884	54.9884	54.9884
Ω_4	101.4533		176.8732	103.1940	102.0666	99.8254	99.7928	99.7477	99.7475	99.7472
Ω_5	154.6768			233.9861	161.1656	158.0084	152.2514	152.0756	151.8493	151.8466

4. Numerical examples

4.1. Example 1: natural frequencies of cantilever stepped beam

A cantilever stepped beam is analyzed in this section. Table 2 summarizes the first five dimensionless natural frequencies obtained with the method developed in this paper and with a finite element model defined in Sap2000 [14] (FEM) using frame elements. The frequency coefficients are also compared with the exact natural frequencies obtained by Rossi et al. [9]. After a convergence analysis it was found that the best results are obtained using 96 frame elements in the Sap2000 model while only 10 polynomials were needed in the approximating functions for the present method.

4.2. Example 2: natural frequencies of clamped–clamped tapered beam

A clamped–clamped tapered beam is analyzed in this section. The first four dimensionless natural frequencies calculated with the method developed in this paper and with a finite element model [14] using 3D solid elements are included in Table 3. In the Sap2000 model [14], after a convergence analysis, 10,240 solid elements are employed, while only 10 polynomials are used in the present method. In addition, the results obtained using the stepped reduction method presented by Tong et al. [2] are shown in that table for comparison purpose. It can be noticed that the present method provides a better agreement to the 3D model results.

5. Free vibration analysis of a bell tower

5.1. Experimental analysis

The algorithm developed in Section 2 is applied here to the dynamical analysis of a real structure: the bell tower of the church "Nuestra Señora Candelaria de la Viña" (Salta, Argentina), built in 1895. Fig. 2 shows a picture of the tower and the side and top layouts.

The numerical models were calibrated using the first natural frequencies of the tower determined from ambient vibration tests. This experimental procedure is based on the determination of the dynamical properties of a structure from the analysis in the frequency domain of the acceleration caused by environmental vibrations and measured at different points of the structure. One advantage of this method is that no special equipment is required to generate the excitement of the structure because the environmental vibrations are always present.

The method takes into account that for structures with low damping and well separated modes of vibration, the peaks in the Fourier transform or power spectral density (PSD) of the measured accelerations (caused by environmental vibrations), match the natural frequencies [10,11].

For the measurement of accelerations a 12-channel digital recorder model K2 of Kinemetrics Inc. and two triaxial accelerometers are used [15]. Fig. 3 shows the layout of the accelerometers located at the top level of the tower (26.8 m high), one is inside the body of the recorder (Accel 1) and the other is independent and connected to it by a cable (Accel 2). Each accelerometer can measure accelerations in three orthogonal directions.

Taking into account the support conditions of the analyzed structure and that in this study the experimental determination of the modal shapes was not necessary; it was considered that the measurement of the accelerations only at the top of the tower was sufficient to define the natural frequencies of the bell tower [10].

Several ambient vibration tests during 30 min each were performed, saving data at a velocity of 200 samples per second. Fig. 4 shows the power spectral density function for acceleration record measures in one test in the North–South direction. The power spectral density was computed using a one-sided autospectral density function [16] implemented in the PSD program version 2.3.2 of Kinemetrics [17].

Table 4 shows the first three natural frequencies obtained from the peaks of the records for the North–South (x) and East–West (y) directions. Even though peaks may be distinguished for higher frequencies, it was considered that due to inevitable noise present in the signal there is some uncertainty in identifying natural frequencies in this range.

5.2. General considerations for the numerical analysis

Two numerical models for obtaining the dynamic behavior of the bell tower are described in this section. The first one is based on the finite element method and the second one in the algorithm proposed in this paper. In the formulation of both models the following considerations are adopted:

(a) The base of the tower is fixed.
(b) The entire tower is built using unreinforced masonry with a uniform density of 1900 kg/m^3 and Poisson ratio equal to 0.15.

The models are defined following the tower geometry. An equivalent global elastic modulus E is obtained by applying the finite element and the analytical methods for different E values until a minimum difference between experimental and numerical fundamental frequencies is obtained [11–13].

Table 2
Dimensionless natural frequencies for stepped beam case.

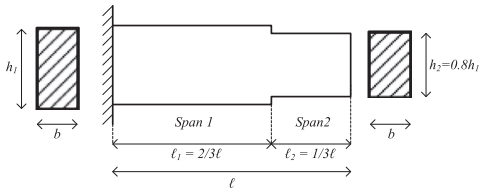

$h_2/h_1 = 0.8$
$b_1 = b_2$
$\ell_1 = \ell = 2/3$
$k = 5/6$
$\nu = 0.3$

$\Omega_i = (\sqrt{\rho_1 A_1 L^4/E_1 I_1})\omega_i$

$\eta_1 = \frac{I_1}{A_1 \ell^2} \therefore h_1 = \sqrt{12\eta_1}\ell$

$\sqrt{\eta_1}$	Frequencies	Exact solution (Rossi et al. [9])	Present method	Sap2000
0.0267	Ω_1	3.80	3.80	3.81
	Ω_2	20.72	20.86	20.88
	Ω_3	51.68	52.04	52.63
	Ω_4	96.39	96.44	99.02
	Ω_5	148.97	149.82	154.16
0.04	Ω_1	3.77	3.77	3.79
	Ω_2	19.80	19.90	20.11
	Ω_3	47.35	47.62	48.92
	Ω_4	84.14	84.21	87.84
	Ω_5	125.06	125.47	131.26

Table 3
Dimensionless natural frequencies for tapered beam case.

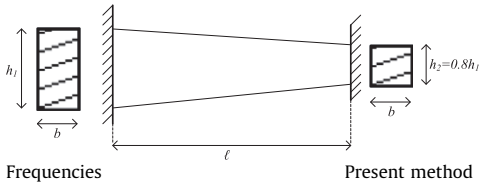

$h_2/h_1 = 0.8$
$b_1 = b_2$
$\kappa = 2/3$
$E = 210$ GPa
$G = 80$ GPa

$\Omega_i = (\sqrt{\rho_1 A_1 L^4/E_1 I_1})\omega_i$

$\eta_1 = \frac{I_1}{A_1 \ell^2} \therefore h_1 = \sqrt{12\eta_1}\ell$

$\sqrt{\eta_1} = 0.02866$

Frequencies	Present method	Sap2000 3D model	Stepped reduction method (Tong et al. [2])
Ω_1	15.65	16.06	15.64
Ω_2	41.07	42.36	40.92
Ω_3	76.07	78.90	75.54
Ω_4	118.22	123.21	116.96

5.3. Finite element model

The modeling of the tower with 3D finite element is performed using SAP2000 [14]. The body of the tower was modeled with 8-node solid elements, while 4 nodes shell elements were used for the dome. The model consists of 8213 nodes, 5563 solid elements, 144 plate elements, resulting in 24,630 degrees of freedom. The minimum difference between the natural frequency measured and calculated is obtained for an elastic modulus of the material equal to 1.96 GPa. This value is between the typical ranges of the elastic modulus of unreinforced masonry. Table 5 shows the frequencies and associated vibration modes of the structure determined with this numerical model.

5.4. Model based on the Ritz method

Fig. 5 and Table 6 summarize the simplifications and parameters adopted for the determination of natural frequencies employing the proposed algorithm. The dome of the tower is represented by means of a lumped mass attached to the tower at the top end by a large rigidity and zero density elements. The magnitude of the lumped mass is determined as the sum of the masses of the dome's architectural and structural components and the length of the element to which it is attached is defined considering the position of the dome mass center. The part of the tower corresponding to the belfry (span 4) contains important openings in their sides, so it is difficult to determine the exact shear correction coefficient. Due to variations of this coefficient have a little influence on the results the coefficient is taken equal to 5/9.

Once the geometry is defined the modulus of elasticity of the model is found following the procedure described in Section 5.2. The natural frequencies corresponding to the first two modes are depicted in Table 7.

5.5. Comparison of experimental and analytical results

Table 8 summarizes the first natural frequencies determined experimentally and those obtained with the numerical models in the *x* direction (North–South). The results obtained with the 3D finite element model allows identifying flexural and rotational modes, by comparing these results with the experimental measurements it is concluded that the first two experimentally determined frequencies correspond to flexural modes, while the third corresponds to a torsional mode. The proposed analytical algorithm considers only displacements in the plane, so it is not possible to determine the rotational modes.

From the analysis of results it can be considered that both methods represent with a good degree of approximation the real dynamic behavior of the tower. The differences between the analytical and experimental results are mainly attributed to the uncertainty about the exact definition of the geometry of the tower, and the lack of uniformity in both the density distribution and the elastic modulus of the material (which are assumed as uniform).

Once the models have been calibrated, the finite element method gives better approximations for the higher modes allowing a more detailed definition of the structural elements and considering a three-dimensional behavior. Despite this, the algorithm based on the Rayleigh–Ritz method has the advantage of requiring much

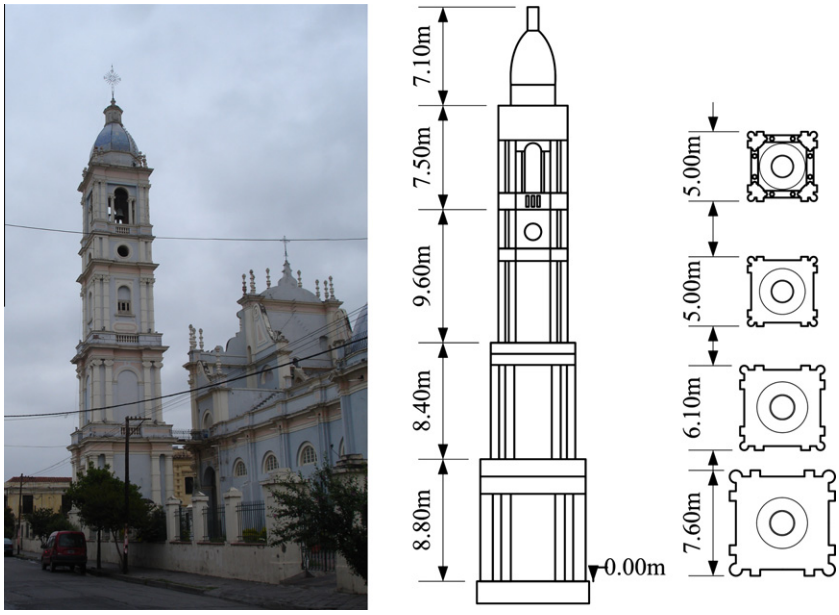

Fig. 2. View and scheme of the bell tower.

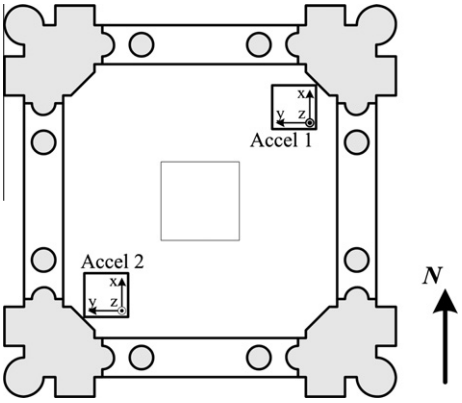

Fig. 3. Arrangement of accelerometers.

less computational effort, both in regard to preprocess (data entry) and the resolution time.

Table 4
Natural frequencies determined experimentally.

Accelerometer	Accel 1		Accel 2	
Direction	*x*	*y*	*x*	*y*
f_1	1.37	1.37	1.37	1.37
f_2	4.10	3.91	4.10	3.91
f_3	5.08	5.08	5.08	5.08

6. Conclusions

A general algorithm, based in the variational Raleigh–Ritz method, for the analysis of thick beams with various complicating effects is presented in this work. The proposed algorithm allows the determination of natural frequencies of beams including shear strains in the kinematics by means of the Timoshenko beam theory. The general algorithm is validated comparing the natural frequencies calculated with exact and approximated results presented in the literature and also with finite element models, showing a rapid convergence and very good agreement.

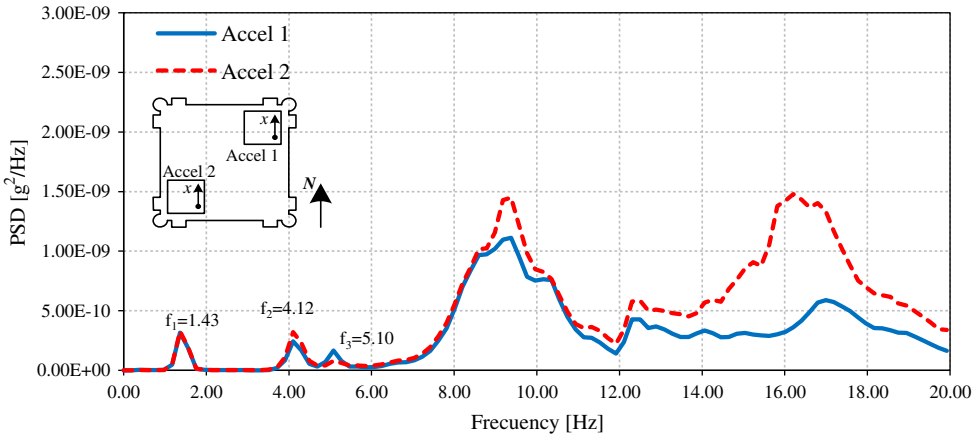

Fig. 4. Power spectral density function for accelerometers in the *x* direction (North–South).

Table 5
Frequencies and modal shapes-3D finite element model.

Mode 1	Mode 2	Mode 3	Mode 4	Mode 5
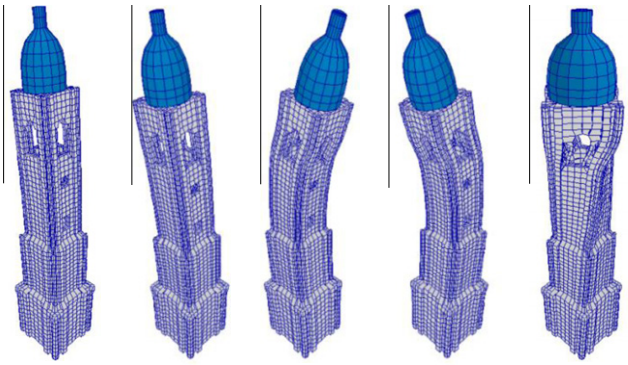				
f_1 = 1.37 Hz Flexural in x	f_2 = 1.37 Hz Flexural in y	f_3 = 4.36 Hz Flexural in x	f_4 = 4.42 Hz Flexural in y	f_5 = 5.25 Hz Torsional

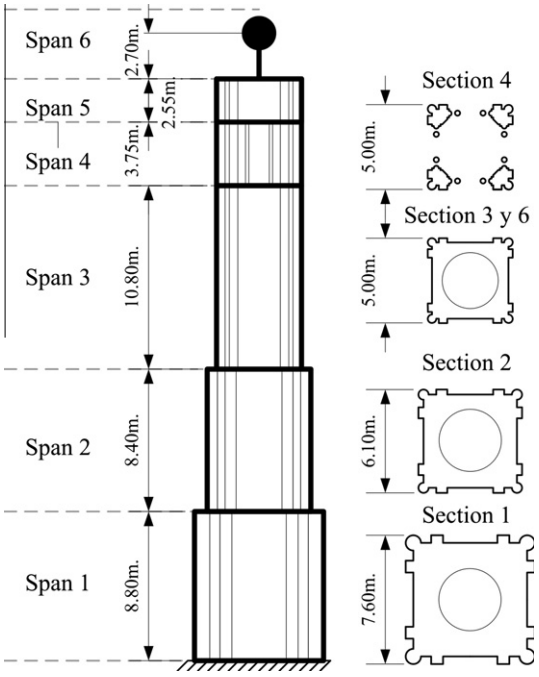

Fig. 5. Simplified scheme of the tower.

Table 6
Sections properties for algorithm analysis.

Span	Area (m^2)	Inertia (m^4)	Density (kg/m^3)	Shear coefficient, κ
6	1×10^6	1×10^6	(23,000 kg concentrate mass)	5/6
5	13.80	36.07	1900	5/9
4	6.26	21.51	1900	5/9
3	13.80	36.07	1900	5/9
2	27.51	86.52	1900	2/3
1	41.28	206.08	1900	17/24

Table 7
Frequencies of the model based on Rayleigh–Ritz method (Hz).

Mode	Frequency
Mode 1	1.37
Mode 2	4.87

Table 8
Comparison of frequencies obtained from different methods (Hz).

Frequency	Experimental	MEF 3D	Raileigh–Ritz
f_1	1.37	1.37	1.37
f_2	4.10	4.36	4.87
f_3	5.08	5.25	–

Additionally, the first natural frequencies of the tower of a church are determined by means of environmental vibration testing using only the acceleration measurement recorded in the highest accessible point. The natural frequencies of the bell tower using the proposed analytical formulation and the finite element method are also obtained. It is noticeable that the proposed method requires less computational work to represent the dynamic behavior of the tower.

Finally, it is important to point out that the proposed algorithm results a useful tool for studying dynamic behavior of beam type structures with precision and simplicity. It should be noted that a good definition of the mechanical and geometrical properties leads to more accurate determination of frequencies employing this method.

References

[1] Farghaly SH. Vibration and stability analysis of Timoshenko beams with discontinuities in cross-section. J Sound Vib 1994;174:591–605.
[2] Tong X, Tabarrok B, Yeh KY. Vibration analysis of Timoshenko beams with non-homogeneity and varying cross-section. J Sound Vib 1995;186:821–35.
[3] Lin HP, Chang SC. Free vibration analysis of multi-span beams with intermediate flexible constraints. J Sound Vib 2005;281:155–69.
[4] Lin HY. Free vibration analysis of a uniform multi-span beam carrying multiple spring-mass systems. J Sound Vib 2007;302:442–56.
[5] Lin HY. Dynamic analysis of a multi-span uniform beam carrying a number of various concentrated elements. J Sound Vib 2007;309:262–75.
[6] Lin HY. On the natural frequencies and mode shapes of a multispan Timoshenko beam carrying a number of various concentrated elements. J Sound Vib 2008;319:593–605.
[7] Nallim LG, Grossi RO. A general algorithm for the study of the dynamical behaviour of beams. Appl Acoust 1999;57:345–56.
[8] Bhat RB. Natural frequencies of rectangular plates using characteristic orthogonal polynomials in Rayleigh–Ritz method. J Sound Vib 1985;102:493–9.
[9] Rossi RE, Laura PAA, Gutierrez RH. A note on transverse vibrations of a Timoshenko beam of non-uniform thickness clamped at one end and carrying a concentrated mass at the other. J Sound Vib 1990;143:491–502.
[10] Barreras FE. Determinación de Características Dinámicas de Estructuras, PhD Thesis, Universidad Politécnica de Cataluña, Barcelona; 1999.
[11] Gentile C, Saisi A. Ambient vibration testing of historic masonry towers for structural identification and damage assessment. Constr Build Mater 2007;21:1311–21.
[12] Ivorra S, Pellarés FJ. Dynamic investigations on a masonry bell tower. Eng Struct 2005;28:660–7.
[13] Russo G, Bergamo O, Damiani L, Lugato D. Experimental analysis of the "Saint Andrea" Masonry Bell Tower I Venice. A new method for the determination of "Tower Global Young's Modulus E. Eng Struct 2010;32:353–60.
[14] SAP2000, User's Manual, Computers and Structures, USA; 1998.
[15] Kinemetrics Inc., Altus Digital Recoreder User's Manual, Kinemetrics Inc., USA; 2002.
[16] Bendat JS, Piersol AG. Random data: analysis and measurement procedures. 2nd ed. New York: John Wiley; 1986.
[17] Kinemetrics Inc., KMI Power Spectral Density, Kinemetrics Inc., USA; 1999.